Scientific Research Publishing

International Journal of Astronomy and Astrophysics, 2025, 15(1), 1-10
https://www.scirp.org/journal/ijaa
ISSN Online: 2161-4725
ISSN Print: 2161-4717

Why Do Galaxies Have Extended Flat Rotation Curves?

Bruce Hoeneisen

Universidad San Francisco de Quito, Quito, Ecuador
Email: bhoeneisen@usfq.edu.ec

How to cite this paper: Hoeneisen, B. (2025) Why Do Galaxies Have Extended Flat Rotation Curves? *International Journal of Astronomy and Astrophysics*, **15**, 1-10.
https://doi.org/10.4236/ijaa.2025.151001

Received: November 30, 2024
Accepted: January 21, 2025
Published: January 24, 2025

Abstract

Recent observations by Mistele *et al.* show that the circular velocity curves of isolated galaxies remain flat out to the largest radii probed so far, *i.e.*, ≈1 Mpc. The velocity decline beyond the expected virial radius is not observed. These results imply that the galaxy halo is in thermal equilibrium even at large radii where particles did not have time to relax. The galaxies must have already formed in the isothermal state. How is this possible? In the present note we try to understand the formation of galaxies with warm dark matter in the expanding universe.

Keywords

Galaxy, Galaxy Formation, Warm Dark Matter, Elliptical Galaxy

1. Introduction

The present study is inspired by weak gravitational lensing measurements that find galaxy circular velocities of test particles to be approximately constant out to the largest radii probed so far, *i.e.*, ≈1 Mpc [1]. The expected virial radius, beyond which the rotation velocity should decline with the Kepler law, is not observed. The flat rotation curves correspond to the "isothermal sphere" with density run $\rho(r) \propto r^{-2}$ with particles with the Maxwell-Boltzmann distribution. Consider a galaxy with a rotation velocity $V(r) = 200$ km/s. The radius r at which the rotation period equals the age of the universe is 0.5 Mpc. So the galaxy at large r has no time to relax to the isothermal equilibrium state: the galaxy must have formed already in this isothermal state. How is this possible?

Figure 1 presents measured total densities $\rho_{\text{tot}}(r)$ and baryon densities $\rho_b(r)$ of the large elliptical galaxy J1313+4615 [2]. The dark matter density is $\rho_h(r) = \rho_{\text{tot}}(r) - \rho_b(r)$. The curves are obtained by integrating numerically

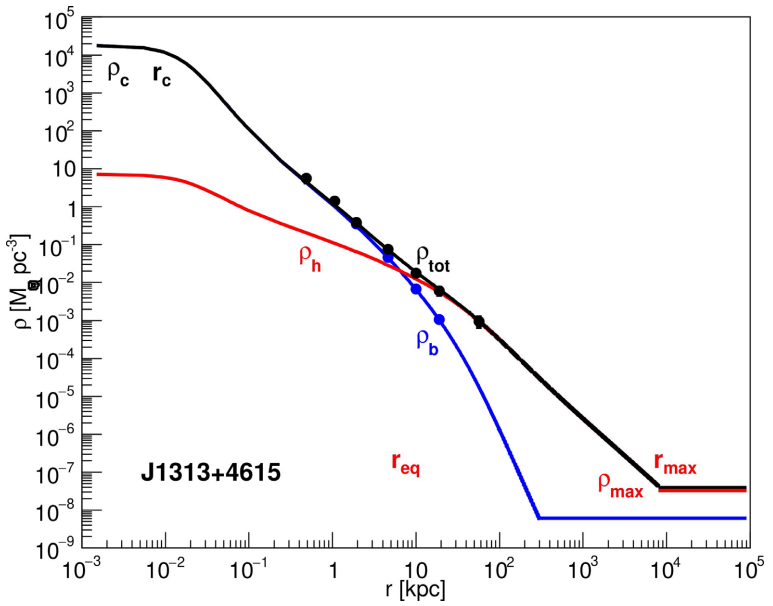

Figure 1. Observed [2] and calculated densities $\rho_{\text{tot}}(r)$, $\rho_b(r)$ and $\rho_h(r)$ of galaxy J1313+4615. The fitted parameters are $\sqrt{\langle v_{rb}^2 \rangle}$, $\sqrt{\langle v_{rh}^2 \rangle}$, $\rho_b(r_{\min})$ and $\rho_h(r_{\min})$ (or $v_{h\text{rms}}(1)$) [3]. Freeing a central black hole mass $M_{BH} = 0$ does not change the fit significantly. The figure defines the core radius r_c and density ρ_c, and the radius $r_{\max}$ with density $\rho_{\max} \equiv \rho(r_{\max}) = \Omega_m \rho_{\text{crit}}$ in this example (or a void, or the halo of a neighboring galaxy).

hydrostatic equations [3] that describe two self-gravitating classical non-relativistic gases, "baryons" and "warm dark matter", in mechanical and, separately, in thermal equilibrium. To start the numerical integration it is necessary to provide four boundary conditions: the root-mean-square radial thermal velocities $\sqrt{\langle v_{rb}^2 \rangle}$ and $\sqrt{\langle v_{rh}^2 \rangle}$ (independent of r) and the core densities $\rho_b(r_{\min})$ and $\rho_h(r_{\min})$, of baryons and of the dark matter halo, respectively. These boundary conditions are varied to minimize a χ^2 between the numerical integration and the data. "Baryons" are mostly neutral and ionized hydrogen and helium during the formation of first generation galaxies, and mostly stars, dust and neutral and ionized gas in later galaxies. The results of the fits are that the radial root-mean-square thermal velocities of dark matter particles and baryons are similar, with

$$\alpha \equiv \frac{\sqrt{\langle v_{rb}^2 \rangle}}{\sqrt{\langle v_{rh}^2 \rangle}} \tag{1}$$

in the approximate range 0.5 to 0.7 in elliptical galaxies [4]. (In spiral galaxies we find α in the approximate range 0.4 to 2.5 [5] as a result of galaxy rotation acquired, presumably, during galaxy collisions and mergers. Rotating galaxies are beyond the scope of the present study.) We note that baryons and warm dark matter have, in general, different temperatures. Therefore, non-gravitational dark matter-baryon interactions can be neglected on galactic scales. Why is α of

order 1? At large radii $r > r_{\rm eq}$ the dark matter density dominates. At small $r < r_{\rm eq}$ the baryon density dominates in large galaxies, while in dwarf galaxies dark matter may dominate even in the core. Excellent fits to the observed density runs of baryons $\rho_b(r)$ and dark matter $\rho_h(r)$ are obtained for dwarf [6], spiral [5] and elliptical [4] galaxies with absolute luminosities that span 4 orders of magnitude, and baryon core densities that span 6 orders of magnitude. These excellent fits justify the hydrostatic equations with $\sqrt{\langle v_{rb}^2 \rangle}$ and $\sqrt{\langle v_{rh}^2 \rangle}$ independent of r. If the galaxies have a third gas, e.g., cold dark matter, current observations can not distinguish it from the baryons since we already obtain excellent fits to the data. An important observation is that the warm dark matter core has an adiabatic invariant $v_{h\rm rms}(1)$ common to dwarf, spiral and elliptical galaxies, even though $\rho_h(r_{\rm min})$ can be orders of magnitude less than $\rho_b(r_{\rm min})$, as in **Figure 1**. We interpret this adiabatic invariant to be of cosmological origin, and identify $v_{h\rm rms}(1)$ with the comoving root-mean-square thermal velocity of the non-relativistic warm dark matter particles in the early universe (see Section 3 below). There is no such observed adiabatic invariant for baryons, possibly because baryons have non-elastic collisions and radiate energy (while the measured $v_{h\rm rms}(1)$ for dark matter has a spread of factor 3 between galaxies, the corresponding $v_{h\rm rms}(1)$ for baryons has a spread of 100 [4]-[6]).

The purpose of the present note is to try to understand **Figure 1** and the isothermal formation of galaxies. These studies are a continuation of [3] and [4].

The basic building block of the galaxy is the isothermal sphere that we briefly review in Section 2. This isothermal sphere grows in thermal equilibrium due to the expansion of the universe (Section 3). The dark matter core radius is determined by the dark matter "warmness" $v_{h\rm rms}(1)$ (Section 4). The preceeding results are valid even if the galaxy has a mix of particles with different masses, so long as collisions are elastic (Section 5). The mix of warm dark matter and baryons, and the effect of inelastic baryon collisions are studied in Section 6. Conclusions follow.

2. The Isothermal Sphere

The flat rotation curves indicate that the galaxy approximates an "isothermal sphere" with particles that obey the Maxwell-Boltzmann distribution [3]. For convenience we briefly review the isothermal sphere. In the first approximation, let us consider a galaxy as a self-gravitating non-relativistic gas of warm dark matter particles of mass m. These particles may be collisionless or may collide elastically. We are interested in spherically symmetric static solutions in mechanical and thermal equilibrium. The corresponding hydrostatic equations are Newton's equation, and the equation of conservation of radial momentum:

$$\nabla \cdot \boldsymbol{g} = \frac{1}{r^2}\frac{\mathrm{d}}{\mathrm{d}r}\left(r^2 g_r\right) = -4\pi G\rho, \quad \nabla P = \frac{\mathrm{d}P}{\mathrm{d}r}\boldsymbol{e}_r = \rho \boldsymbol{g}, \quad P \equiv \left\langle v_r^2 \right\rangle \rho, \tag{2}$$

where the mean-square dark matter particle radial velocity $\langle v_r^2 \rangle$ is independent

of the radial coordinate r, *i.e.*, is isothermal. The only solution with density run $\rho(r) \propto r^{-n}$ and $\langle v_r^2 \rangle \propto r^{-k}$ is

$$\rho(r) = \frac{\langle v_r^2 \rangle}{2\pi G r^2} \equiv \rho_c \left(\frac{r_c}{r} \right)^2 \tag{3}$$

with $k = 0$. Here we have defined $\rho_c r_c^2$. The velocity of a test particle in a circular orbit is $V = \sqrt{2\langle v_r^2 \rangle}$. Observed flat rotation curves at large r indicate that $\langle v_r^2 \rangle$ is independent of r and $\rho(r) \propto r^{-2}$, *i.e.*, the galaxy halo is an isothermal sphere at large r. The gravitational potential per unit mass with respect to a radial coordinate r_c is

$$\Phi(r) \equiv -\int_{r_c}^{r} g_r \mathrm{d}r = 2\langle v_r^2 \rangle \ln\left(\frac{r}{r_c} \right). \tag{4}$$

The general solution of (2) depends on two boundary conditions, *i.e.*, the core density ρ_c at $r \to 0$, and $\sqrt{\langle v_r^2 \rangle}$ (and the mass of a central black hole that we will not consider here). In other words, to initiate the numerical integration of (2) the boundary conditions $\rho(r_{\min})$ and $\sqrt{\langle v_r^2 \rangle}$ are required. Here we will be interested in an approximate analytical solution defined by two asymptotes: the density (3) for $r \gg r_c$, and $\rho(r) = \rho_c$ for $r \ll r_c$. These two asymptotes meet at the core radius

$$r_c = \sqrt{\frac{\langle v_r^2 \rangle}{2\pi G \rho_c}}. \tag{5}$$

Note that $\langle v_r^2 \rangle$ is defined at large r.

The energy of one particle at r, with total momentum $p = m\sqrt{\beta v_r^2}$, is

$$E = \frac{1}{2} m\beta v_r^2 + 2m\langle v_r^2 \rangle \ln\left(\frac{r}{r_c} \right). \tag{6}$$

$\beta = 1$ if dark matter is collisionless and velocities are radial, or $\beta = 3$ if dark matter particles have elastic collisions and the velocities have become isotropic.

The mean number of particles (<1) in a quantum state in the non-degenerate gas is proportional to the Boltzmann factor $\exp(-E/kT)$. kT is a constant (independent of r), with units Joule, called "temperature". The number of quantum states of a particle in the phase space volume $\mathrm{d}^3\boldsymbol{r}\mathrm{d}^3\boldsymbol{p}$ is proportional to this volume. The number of particles per unit phase space volume is

$$\frac{\mathrm{d}n}{\mathrm{d}^3\boldsymbol{r}\mathrm{d}^3\boldsymbol{p}} \propto \exp\left(-\frac{E}{kT} \right). \tag{7}$$

The mean-square total velocity $\langle v^2 \rangle$ obtained from (7) satisfies these equations:

$$\frac{1}{2} m\langle v^2 \rangle = \frac{1}{2} m\beta \langle v_r^2 \rangle = \frac{3}{2} kT, \tag{8}$$

independently of r. The energy of each particle in $\mathrm{d}n$ is (6). Since the exponential in (7) separates into factors that depend either on r or on p, the density of

the gas is $\propto r^{-2}$ if $kT = m\langle v_r^2 \rangle$, so $\beta = 3$. $\beta = 1$ is in disagreement with thermal equilibrium and the observed flat rotation curves at large r. We conclude that dark matter particles have elastic collisions, and velocities become isotropic at least in the core. In each volume element $\mathrm{d}^3\boldsymbol{r}$, the particle velocities have the same Maxwell distribution with the same kT and same $\langle v_r^2 \rangle$ independent of r.

3. The Isothermal Sphere in an Expanding Universe

A homogeneous expanding universe has a matter density:

$$\rho(a) = \frac{\Omega_m \rho_{\mathrm{crit}}}{a^3}, \tag{9}$$

where $a(t)$ is the expansion parameter (normalized to $a(t_0) = 1$ at the present time t_0). We assume matter dominates so $a(t) \propto t^{2/3} \propto H^{-2/3} \propto \rho^{-1/3}$. The dark matter particle root-mean-square thermal velocity at expansion parameter a is

$$v_{h\mathrm{rms}}(a) = \frac{v_{h\mathrm{rms}}(1)}{a}. \tag{10}$$

$v_{h\mathrm{rms}}(1)$ is the adiabatic invariant that defines how "warm" the dark matter is.

Consider a positive density perturbation in a homogeneous expanding universe. An observer in this density peak "sees" dark matter expand adiabatically, reach maximum expansion, and then contract into the core of a galaxy. By fitting galaxy rotation curves (or galaxy density runs) it is possible to measure $\langle v_r^2 \rangle = V^2/2$ at large r, and $\rho_c = 3(\mathrm{d}V/\mathrm{d}r)^2/(4\pi G)$ at small r, and obtain

$$v'_{h\mathrm{rms}}(1) = \sqrt{3\langle v_r^2 \rangle}\left(\frac{\Omega_c \rho_{\mathrm{crit}}}{\rho_c}\right)^{1/3}. \tag{11}$$

If the expansion and contraction were free of relaxation and rotation, $v'_{h\mathrm{rms}}(1)$ would be equal to the adiabatic invariant $v_{h\mathrm{rms}}(1)$. However, due to relaxation and rotation, in general $v'_{h\mathrm{rms}}(1) \gtrsim v_{h\mathrm{rms}}(1)$ [7]. The measured width of the distribution of $v'_{h\mathrm{rms}}(1)$ determines the contribution from relaxation and rotation (a factor γ between 1 and ≈3), and the lower bound of the measured distribution determines the adiabatic invariant $v_{h\mathrm{rms}}(1)$. Fits to dwarf galaxy rotation curves, with a core density dominated by dark matter, obtain $v_{h\mathrm{rms}}(1) = 406 \pm 69$ m/s [6]. A summary of *measurements* that justify the interpretation that $v_{h\mathrm{rms}}(1)$ is of cosmological origin is presented in [7].

At $r > r_c$ the halo of the isolated galaxy approaches the density run $\rho(r) \propto r^{-2}$ until it reaches, in our example, the mean density of the expanding universe (9) (or a void, or the halo of a neighboring galaxy). This behavior can be seen by solving hydrodynamical equations [3]. The galaxy halo reaches $\rho(a_{\max}) \equiv \rho_{\max}$ at

$$r_{\max} = r_c\left(\frac{\rho_c}{\rho_{\max}}\right)^{1/2}. \tag{12}$$

At $a_{\max}$, the Hubble expansion parameter is

$$H_{\max} = H_0 \sqrt{\frac{\rho(a_{\max})}{\rho_{\text{crit}}}} = H_0 \sqrt{\Omega_m} a_{\max}^{-3/2}. \tag{13}$$

Note (from (5), (12), (13) and $\rho_{\text{crit}} = 3H_0^2/(8\pi G)$) that the expansion velocity at $r_{\max}$ is independent of $a_{\max}$:

$$H_{\max} r_{\max} \approx \sqrt{\frac{4}{3}} \sqrt{\langle v_r^2 \rangle}. \tag{14}$$

The ≈ symbol is due to the inhomogeneity of the universe density during galaxy formation. In (14) we are neglecting the dark matter thermal velocity $v_{h\text{rms}}(a_{\max}) = v_{h\text{rms}}(1)/a_{\max}$ at $a_{\max}$.

The particles that are captured at $r_{\max}$ by the growing galaxy halo form a galaxy in thermal equilibrium if the expansion velocity $H_{\max} r_{\max} \approx \sqrt{3\langle v_r^2 \rangle}$. These particles populate the tail end of the Boltzmann distribution. We note that $M(r) \propto r$, so the fraction of particles with energies

$$E = \frac{1}{2} m \cdot 3 \langle v_r^2 \rangle + 2m \langle v_r^2 \rangle \ln\left(\frac{r}{r_c}\right) \tag{15}$$

in the interval corresponding to r and $r + \mathrm{d}r$, is proportional to $\mathrm{d}r$.

We also note that $r_{\max}$ grows in proportion to $a_{\max}^{3/2}$ while the separation between neighboring galaxies grows slower (in proportion to $a_{\max}$), so the universe becomes filled with galaxy halos leaving little intergalactic medium.

In conclusion, the halo formation is approximately isothermal without the need for relaxation: the galaxy halo radius grows populating the tail of the Maxwell-Boltzmann distribution (7).

4. The Galaxy Core

Let us consider a dwarf galaxy with a core density dominated by warm dark matter. We neglect dark matter particle collisions during the first orbit. A dark matter particle orbit has a distance of closest approach to the galaxy center $r_{\min}$ that is obtained from $r_{\max}$, the transverse thermal velocity $\approx \pm v_{h\text{rms}}(1)/a_{\max}$ at $r_{\max}$, the velocity $\approx \sqrt{\langle v_r^2 \rangle (\beta + 4\ln(r_{\max}/r_c))}$ in the core of a dark matter particle captured at $r_{\max}$, and by conservation of angular momentum:

$$r_{\min} = \pm r_c \frac{v_{h\text{rms}}(1)}{v'_{h\text{rms}}(1)} \cdot f\left(\frac{\rho_c}{\rho_{\max}}\right)^{1/3}. \tag{16}$$

The function

$$f\left(\frac{\rho_c}{\rho_{\max}}\right) \equiv \left(\frac{\rho_c}{\rho_{\max}}\right)^{1/6} \frac{1}{\sqrt{\beta + 2\ln(\rho_c/\rho_{\max})}} \tag{17}$$

lies in the range 0.5 to 1.4 for $\rho_{\max}/\rho_c$ in the range 10 to 10^5, and β either 1 or 3. So, the core radius $|r_{\min}| \approx r_c$ implies that the measured $v'_{h\text{rms}}(1)$ in the core of a galaxy is approximately equal to adiabatic invariant $v_{h\text{rms}}(1)$ defined in (10), and so is indeed of cosmological origin (as argued in Section 3 and in [3], and as

confirmed by measurements summarized in [7]).

5. The Iso-$\langle v_r^2 \rangle$ Sphere

So far, we have considered a gas of particles of mass m. Let us now consider a gas with a mix of particles with different masses. We still consider the case of particles that have elastic collisions. The results of sections 2 and 3 remain valid, except that E and kT in (7) are proportional to the particle masses, see (6) and (8). The Maxwell-Boltzmann distribution of velocities remains unchanged because E/kT is independent of mass. Note that, if particles are unable to exchange energy, particles of different masses have different temperatures. However, in equilibrium $\langle v_r^2 \rangle$ remains the same for all particles, independently of their mass, and independent of r. In this case the "isothermal sphere" should more properly be called the "iso-$\langle v_r^2 \rangle$ sphere". In the limit of baryons with elastic collisions, $\alpha = 1$ (with α defined in (1)).

6. Adding Baryons

Let us consider the galaxy as a self-gravitating mix of two gases: warm dark matter that has elastic collisions, and baryons that have inelastic collisions. The hydrostatic equations are two sets of equations like (2) separately for warm dark matter and baryons, with $\boldsymbol{g} = \boldsymbol{g}_h + \boldsymbol{g}_b$ [3]. To start the numerical integration it is necessary to provide four boundary conditions: $\sqrt{\langle v_{rb}^2 \rangle}$, $\sqrt{\langle v_{rh}^2 \rangle}$, $\rho_b(r_{\min})$ and $\rho_h(r_{\min})$. These four parameters need to be taken from observations, predictions or simulations. Excellent fits to the data of dwarf, spiral and elliptical galaxies justify taking $\sqrt{\langle v_{rb}^2 \rangle}$ and $\sqrt{\langle v_{rh}^2 \rangle}$ independent of r. The asymptotic solutions of the hydrostatic equations are:

$$\rho_b(r): \quad \rho_b(r_{\min}) \quad \to \quad \frac{\langle v_{rb}^2 \rangle}{2\pi G r^2} \quad \to \quad \propto \frac{1}{r^{2/\alpha^2}}, \tag{18}$$

$$\rho_h(r): \quad \rho_h(r_{\min}) \quad \to \quad \propto \frac{1}{r^{2\alpha^2}} \quad \to \quad \frac{\langle v_{rh}^2 \rangle}{2\pi G r^2}. \tag{19}$$

α is defined in (1). These asymptotic solutions allow an understanding of **Figure 1**. Note that in the limit $\alpha = 1$ we recover the "iso-$\langle v_r^2 \rangle$ sphere". Why is $\alpha < 1$ in elliptical galaxies [4]? There are two reasons. For first generation galaxies, the "baryons", mostly hydrogen and helium, become neutral and decouple from photons at redshift $z_{\text{eq}} = 1090$, and so for first generation galaxies $v_{b\text{rms}}(1) \approx 8\ \text{m/s} \ll v_{h\text{rms}}(1) \approx 406\ \text{m/s}$. Hydrodynamical equations show that the collapsing warmer dark matter develops a core and forms later than the colder baryons [3]. The second reason for $\alpha < 1$ is that baryons have inelastic collisions and gradually migrate towards the center of the galaxy halo. In large galaxies, the core density is dominated by baryons. The baryon core radius determines, and is equal to, the dark matter core radius. The shrinking baryon core radius compresses the warm dark matter in the core conserving the adiabatic invariant

$v_{h\mathrm{rms}}(1)$ (see Figure 1).

Photometric and spectroscopic galaxy observations may obtain the redshift z, the stellar mass M_*, and the baryon velocity dispersion $\sqrt{\langle v_{rb}^2 \rangle}$. If detailed density runs $\rho_b(r)$ are observable, as in Figure 1, then the break radius r_{eq} is obtained, and a redundant measurement of $\sqrt{\langle v_{rb}^2 \rangle}$ is possible:

$$\rho_{\mathrm{eq}} \approx \frac{\langle v_{rb}^2 \rangle}{2\pi G r_{\mathrm{eq}}^2}. \tag{20}$$

Integrating the asymptotes (18) obtains

$$M_* = \frac{2-2\alpha^2}{2-3\alpha^2} \cdot \frac{2\langle v_{rb}^2 \rangle}{G} r_{\mathrm{eq}} \tag{21}$$

(valid for $\alpha^2 < 2/3$). As a first approximation we may take $\alpha \approx 0.6$, so (21) is another constraint between r_{eq} and $\langle v_{rb}^2 \rangle$.

The adiabatic invariant places another constraint between the boundary conditions:

$$v'_{h\mathrm{rms}}(1) = \sqrt{3\langle v_{rh}^2 \rangle} \left(\frac{\Omega_c \rho_{\mathrm{crit}}}{\rho_h(r_{\min})} \right)^{1/3} \equiv \gamma v_{h\mathrm{rms}}(1), \tag{22}$$

with $v_{h\mathrm{rms}}(1) = 406 \pm 69$ m/s [7], and the relaxation factor γ observed to be in the approximate range from 1 to 3.

Galaxy stellar masses M_* may be related to primordial linear density perturbations of total (dark matter plus baryon) mass M. This mass M is defined by the Press-Schechter formalism with a gaussian window function and a power spectrum $P(k)\tau^2(k)$ with a cut-off factor $\tau^2(k)$ due to the warm dark matter free-streaming [8]-[10]. These Press-Schechter predictions, or their ellipsoidal collapse extensions pioneered by R.K. Sheth and G. Tormen [11] [12], are in excellent agreement with galaxy stellar mass M_* and ultra-violet luminosity distributions in a wide range of redshifts [9]. Comparing these predictions with observations we obtain the following approximate relation [9]:

$$\frac{M}{M_\odot} \approx 10^{1.5} \frac{M_*}{M_\odot}. \tag{23}$$

An empirical constraint between M_* and V is the baryonic Tully-Fisher relation for isolated galaxies [1]. Similar relations are obtained from (20) and (21):

$$M_* \propto V^2 r_{\mathrm{eq}} \propto \frac{V^3}{\sqrt{\rho_{\mathrm{eq}}}}. \tag{24}$$

7. Conclusions

The observed extended flat rotation curves of galaxies [1] indicate that galaxies are approximately isothermal spheres with particles obeying the Maxwell-Boltzmann distribution [3]. The dark matter particles are collisional and these collisions are elastic. The galaxies do not have time to relax to the isothermal equilibrium state, so they must have formed already in this state. This isothermal

formation is due to the growing galaxy halo with density run $\rho(r) \propto r^{-2}$ at large r, and the expansion of the universe. The particles falling into the growing galaxy halo potential well populate the tail end of the Maxwell-Boltzmann distribution. The halos grow until they meet voids or halos of neighboring galaxies.

The dark matter core radius is determined by the "warmness" $v_{h\mathrm{rms}}(1)$ of the dark matter. This adiabatic invariant is of cosmological origin, as shown by arguments in Section 3 and in [3], by measurements summarized in [7], and by the observed dwarf galaxy dark matter cores as shown in section 4. The measured warm dark matter adiabatic invariant $v_{h\mathrm{rms}}(1)$ happens to be in agreement with the "no freeze-in and no freeze-out" scenario of scalar dark matter coupled to the Higgs boson [7].

"Baryons" have lower thermal velocities than dark matter during the formation of first generation galaxies, and have inelastic collisions, radiate energy, and migrate towards the bottom of the gravitational potential well, so $\alpha \equiv \sqrt{\langle v_{rb}^2 \rangle / \langle v_{rh}^2 \rangle}$ becomes less than 1.

In large galaxies, the core baryon density may dominate the core warm dark matter density by several orders of magnitude, as shown in **Figure 1**, yet the measured adiabatic invariant in the warm dark matter core remains invariant within uncertainties and relaxation corrections [4].

Note that warm dark matter simulations should not neglect the thermal velocity if the galaxy core is of interest. If the intergalactic medium is of interest, as in studies of the Lyman-α forest of quasar light, it is necessary to cross-check that the simulations obtain the observed extended galaxy halos with flat rotation curves [1], since these halos leave little space to the "intergalactic medium".

Acknowledgements

I thank Karsten Müller for his early interest in this work and for many useful discussions.

Conflicts of Interest

The author declares no conflicts of interest regarding the publication of this paper.

References

[1] Mistele, T., McGaugh, S., Lelli, F., Schombert, J. and Li, P. (2024) Radial Acceleration Relation of Galaxies with Joint Kinematic and Weak-Lensing Data. *Journal of Cosmology and Astroparticle Physics*, **2024**, Article 20. https://doi.org/10.1088/1475-7516/2024/04/020

[2] Shajib, A.J., Treu, T., Birrer, S. and Sonnenfeld, A. (2021) Dark Matter Haloes of Massive Elliptical Galaxies at z~0.2 Are Well Described by the Navarro–Frenk–White Profile. *Monthly Notices of the Royal Astronomical Society*, **503**, 2380-2405. https://doi.org/10.1093/mnras/stab536

[3] Hoeneisen, B. (2023) Understanding the Formation of Galaxies with Warm Dark Matter. *Journal of Modern Physics*, **14**, 1741-1754. https://doi.org/10.4236/jmp.2023.1413103

[4] Hoeneisen, B. (2024) Understanding Elliptical Galaxies with Warm Dark Matter. *Physics of the Dark Universe*, **46**, Article 101643. https://doi.org/10.1016/j.dark.2024.101643

[5] Hoeneisen, B. (2019) The Adiabatic Invariant of Dark Matter in Spiral Galaxies. *International Journal of Astronomy and Astrophysics*, **9**, 355-367.

[6] Hoeneisen, B. (2022) Measurement of the Dark Matter Velocity Dispersion with Dwarf Galaxy Rotation Curves. *International Journal of Astronomy and Astrophysics*, **12**, 363-381. https://doi.org/10.4236/ijaa.2022.124021

[7] Hoeneisen, B. (2024) Measurements of the Dark Matter Mass, Temperature and Spin. *International Journal of Astronomy and Astrophysics*, **14**, 184-202. https://doi.org/10.4236/ijaa.2024.143012

[8] Press, W.H. and Schechter, P. (1974) Formation of Galaxies and Clusters of Galaxies by Self-Similar Gravitational Condensation. *The Astrophysical Journal*, **187**, 425-438. https://doi.org/10.1086/152650

[9] Hoeneisen, B. (2024) Are James Webb Space Telescope Observations Consistent with Warm Dark Matter? *International Journal of Astronomy and Astrophysics*, **14**, 45-60. https://doi.org/10.4236/ijaa.2024.141003

[10] Hoeneisen, B. (2022) Measurement of the Dark Matter Velocity Dispersion with Galaxy Stellar Masses, UV Luminosities, and Reionization. *International Journal of Astronomy and Astrophysics*, **12**, 258-272. https://doi.org/10.4236/ijaa.2022.123015

[11] Sheth, R.K. and Tormen, G. (1999) Large-scale Bias and the Peak Background Split. *Monthly Notices of the Royal Astronomical Society*, **308**, 119-126. https://doi.org/10.1046/j.1365-8711.1999.02692.x

[12] Sheth, R.K., Mo, H.J. and Tormen, G. (2001) Ellipsoidal Collapse and an Improved Model for the Number and Spatial Distribution of Dark Matter Haloes. *Monthly Notices of the Royal Astronomical Society*, **323**, 1-12. https://doi.org/10.1046/j.1365-8711.2001.04006.x